

Supporting Information

Sample-to-answer COVID-19 nucleic acid testing using a low-cost centrifugal microfluidic platform with bead-based signal enhancement and smartphone read-out

*Ruben R. G. Soares^a; Ahmad S. Akhtar^a; Inês F. Pinto^a; Noa Lapins^a; Donal Barrett^b;
Gustaf Sandh^c; Xiushan Yin^{b, d, e}; Vicent Pelechano^b; Aman Russom^{a, f*}*

^a KTH Royal Institute of Technology, Division of Nanobiotechnology, Department of Protein Science, Science for Life Laboratory, Solna, Sweden

^b Science for Life Laboratory, Department of Microbiology, Tumor and Cell Biology, Karolinska Institutet, Solna, Sweden

^c Department of Clinical Microbiology, Karolinska University Hospital, Stockholm, Sweden.

^d Applied Biology Laboratory, Shenyang University of Chemical Technology, Shenyang, China

^e Biotech and Biomedicine Science Co. Ltd, Shenyang, China

^f AIMES - Center for the Advancement of Integrated Medical and Engineering Sciences at Karolinska Institutet and KTH Royal Institute of Technology, Stockholm, Sweden

* Contact author:

aman@kth.se (A. Russom)

Table of Contents

Figure S1. Post-PCR enrichment of amplicons in agarose beads	3
Figure S2. Schematics of bead selectivity after LAMP and PCR amplification	5
Figure S3. Detailed dimensions of disc microchannels	6
Figure S4. Detailed view of centrifugal platform	7
Figure S5. Schematics of laser incidence angle	8
Table S1. Clinical sample data	9
Figure S6. Data of clinical sample measurements using the iLACO primers	12
Figure S7. As1e and iLACO primer LAMP with and without NBNM beads	13
Figure S8. Raw data of clinical sample measurements using As1e primers.....	14
Figure S9. Representative smartphone photos of negative and positive clinical samples	15
Table S2. Cost estimate of key components in the integrated platform	16

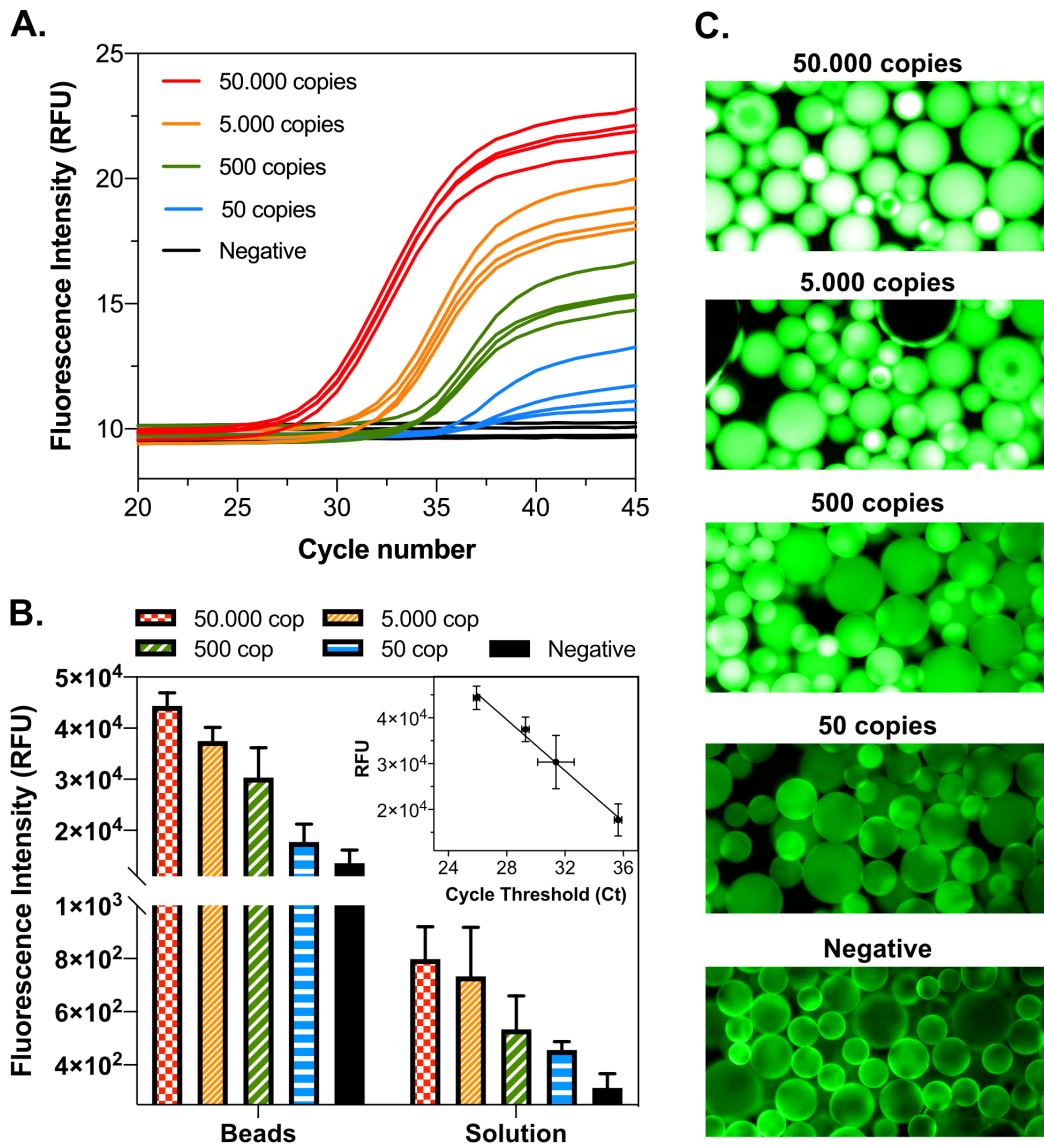


Figure S1. Proof-of-concept of PCR amplicon enrichment on N-benzyl-N-methylethanolamine beads. Synthetic SARS-CoV-2 full genomic RNA (MN908947.3, Twist Bioscience) was spiked at a total of 50 to 50,000 copies per 25 μ L reaction mix containing 1x TaqMan FAST Virus 1-step MM (Thermo Fisher Scientific), 0.6 μ M forward primer (5'-GTG ARA TGG TCA TGT GTG GCG G-3'), 0.8 μ M reverse primer (5'-CAR ATG TTA AAS ACA CTA TTA GCA TA-3') and 0.2 μ M of molecular beacon probe 1 (5'-FAM-CAG GTG GAA CCT CAT CAG GAG ATG C-BHQ_1-3') and 2 (5'-FAM-CCA GGT GGW ACR TCA TCM GGT GAT GC-BHQ_1-3'). The mixture was first incubated for 5 min at 50 $^{\circ}$ C for reverse transcription, denatured for 20 s at 95 $^{\circ}$ C and subjected to a series of 45 cycles of 3 s at 95 $^{\circ}$ C and 30 s at 60 $^{\circ}$ C. The amplification generates a 100 bp long amplicon. A- RT-PCR with increasing RNA copy numbers in solution, measured using a micPCR magnetic induction cyler (BMS, Australia). Each

viral copy titer was measured in quadruplicate. B- Fluorescence intensity measured on Cpto Adhere beads, or solution upstream of the beads after flowing 10 μ L of the pre-amplified mixture (after the 45 amplification cycles in A) through the bead-packed microchannel. Both fluorescence intensity on the beads and in solution were measured using fluorescence microscopy and ImageJ software (NIH, USA) by measuring the grey scale intensity in both regions (16-bit images). The beads provide an increase of \sim 100-fold in fluorescence signal intensity. Vertical and horizontal error bars correspond to the standard deviation of 4 independent PCR amplification and bead-capture experiments. The inset plot shows the correlation between cycle threshold values of the tested viral loads and fluorescence intensity measured on the beads. C- Microscopy images of the beads with increasing copy numbers of SARS-CoV-2 genomic RNA (initial copy numbers before PCR).

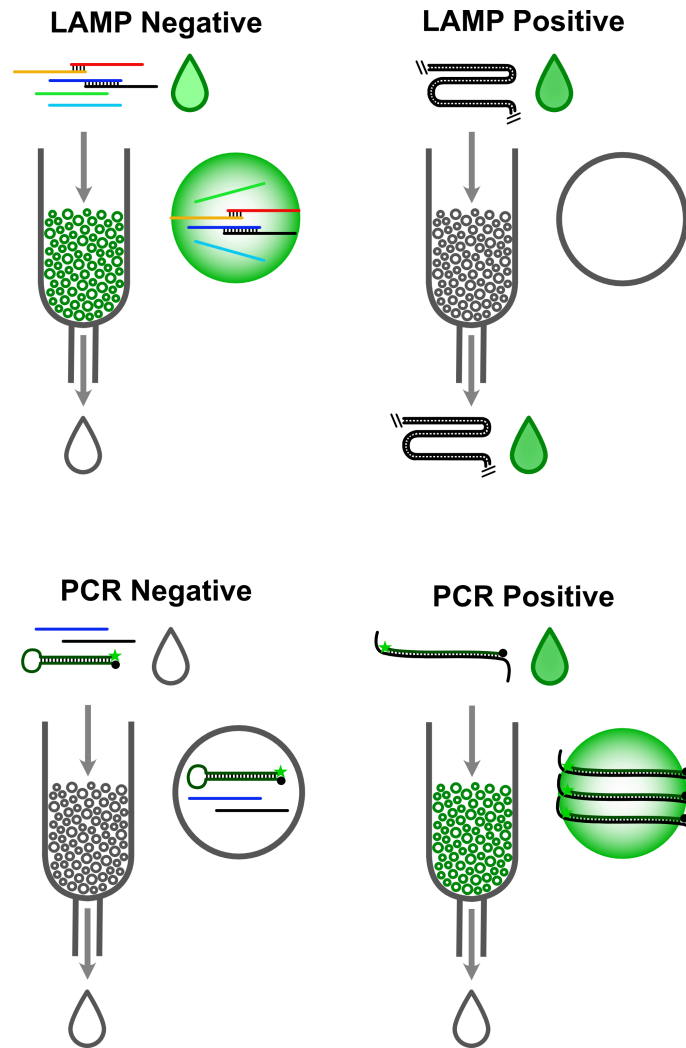


Figure S2. Schematics of the bead capture selectivity in the presence of positive or negative samples amplified with LAMP or PCR. In the case of LAMP, the fluorescence is generated by a dsDNA fluorescent intercalator (e.g. SYBR green I). For PCR, the fluorescence is generated using a molecular beacon (e.g. FAM-BHQ-1 pair). In the tested setup, the PCR amplicon has a length of 100 bp and is able to effectively penetrate the pores of the agarose beads. Green droplets indicate strongly fluorescent solutions, while white droplets indicate non-fluorescent or weakly fluorescent solutions.

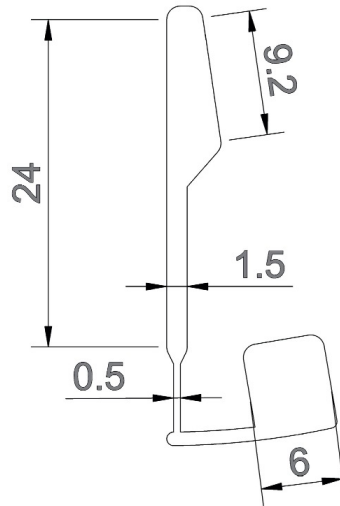


Figure S3. Detailed dimensions (parallel to the rotation axis) of the microchannels drilled on the discs. All values are in mm units. The depth of the channel is 400 μm except at the interface between the 0.5 mm and 6 mm wide regions, where the depth is 50 μm .

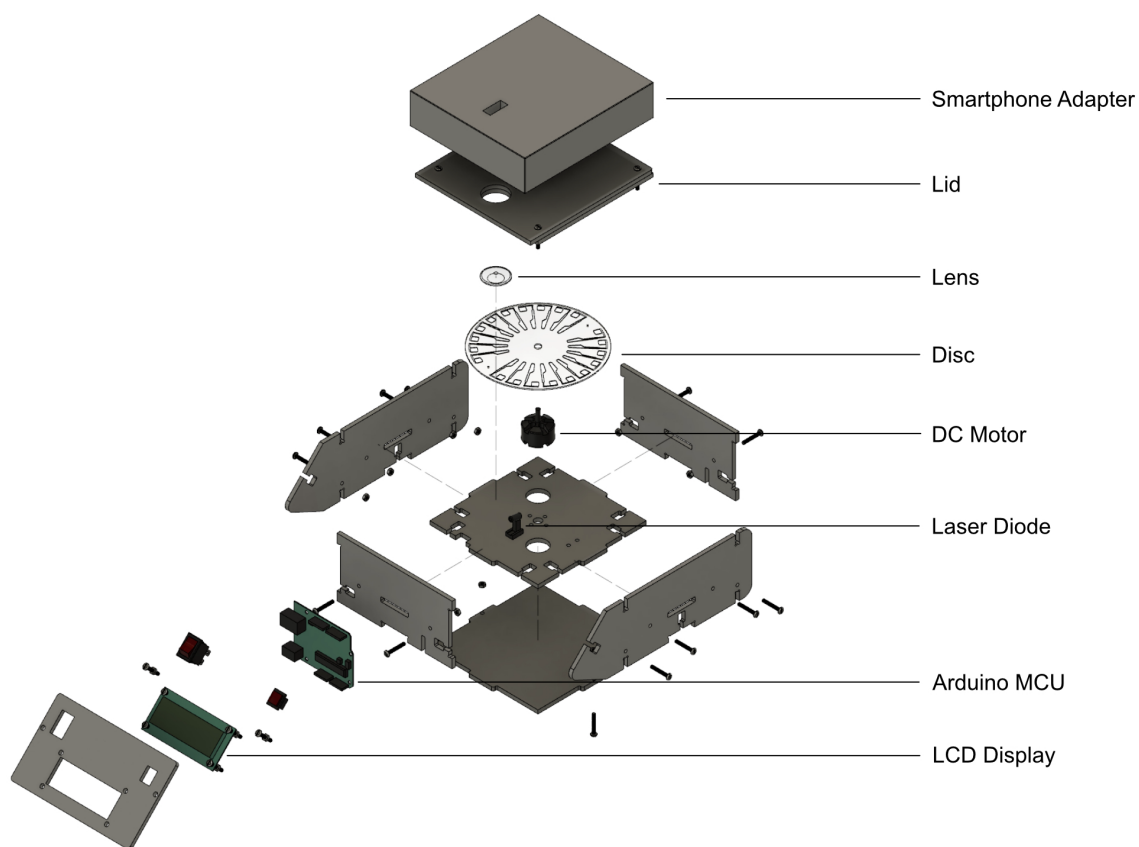


Figure S4. Exploded view of the centrifugal platform. The smartphone adapter design depends on the specific position of the camera being used and can be adapted to ensure an optimal focal distance when measuring the fluorescence signal on the microchannels. A Kapton™ 100 µm thick polyimide film is attached between the lens and the disc to block the excitation light from the laser diode.

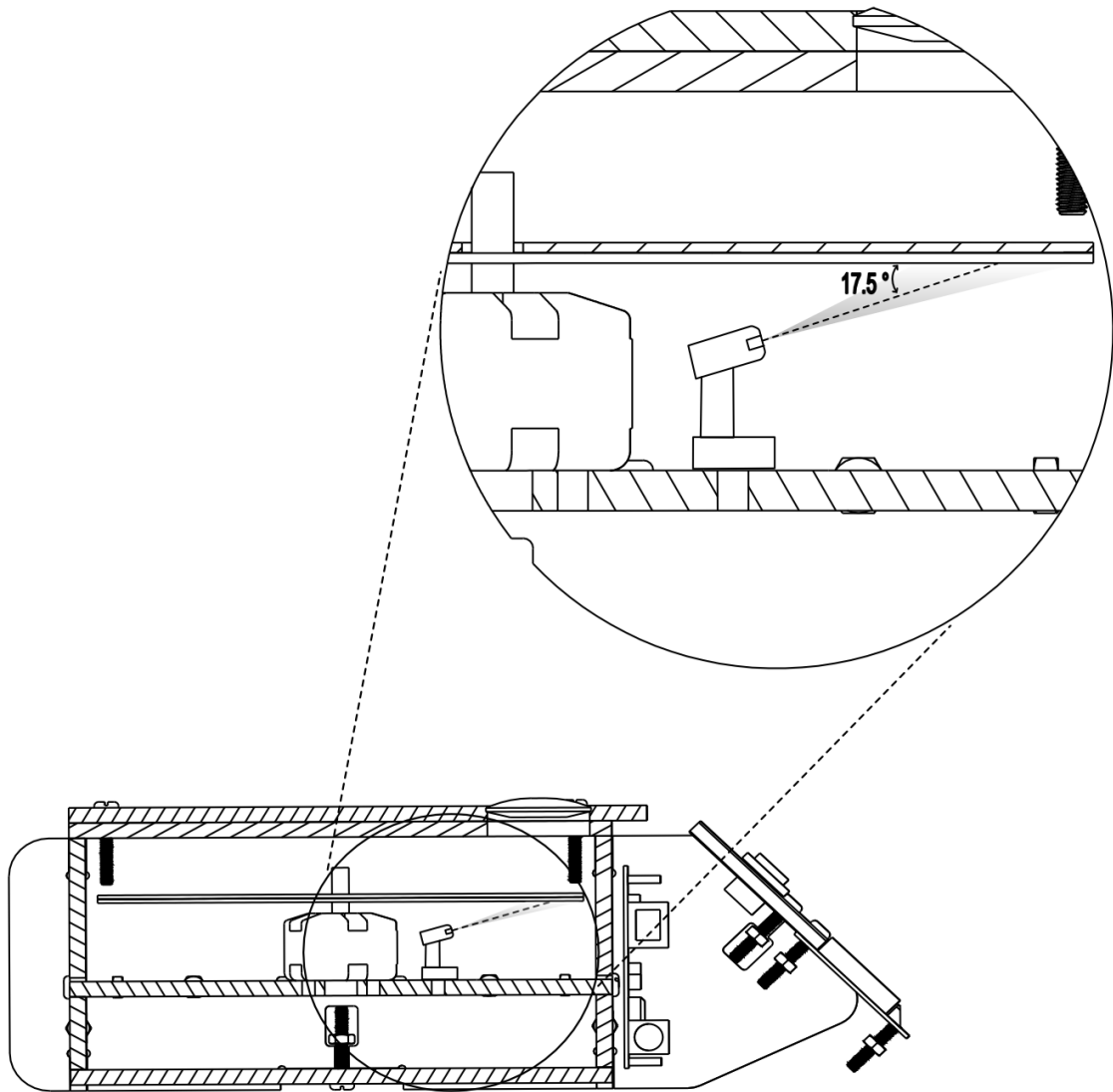


Figure S5. Position and incidence angle of the laser light relative to the disc. The light from the laser has a perpendicular beam divergence of 25° (FWHM) and a parallel beam divergence of 11° . The higher perpendicular divergence ensures illumination of the entire solution and bead region along the microchannels.

Table S1. Nasopharyngeal swab samples analysed using Cepheid GeneXpert targeting E and N genes. “Average Ct” refers to the average of both E and N gene Ct values. “Medium” refers to the collection tube used to store the nasopharyngeal swab samples prior to analysis. Virocult transport tubes contained liquid Virocult medium and both Transwab and ESwab tubes contained liquid Amies medium. Sample ID codes refer to very high viral load (V), high viral load (H), medium viral load (M), low viral load (L), very low viral load (VL) and PCR-negative samples (N). All samples were collected at Karolinska University Hospital (Huddinge) from patients having symptoms attributable to a possible SARS-CoV-2 infection. Sample IDs identified with an asterisk were tested using the iLACO primer set. All remaining samples were tested with the As1e primer set.

Sample ID	Ct E	Ct N2	Average Ct	Medium
V1*	11	13.5	12.3	Virocult
V2*	12.2	14.5	13.4	Virocult
V3*	13.5	15	14.3	Transwab
V4*	13.3	15.8	14.6	Transwab
V5*	13.7	15.4	14.6	Transwab
H1*	14.3	16.3	15.3	Virocult
H2*	15.6	17.8	16.7	Virocult
H3*	16.9	18.8	16.9	Transwab
H4*	17.1	18.9	18.0	Transwab
H5*	17.6	19.8	18.7	Virocult
H6	14,5	16,9	15,7	Virocult
H7	14,5	17,2	15,85	Virocult
H8	16,2	18,5	17,35	Virocult
H9	16,3	18,4	17,35	Virocult
H10	16,5	18,3	17,4	Virocult
H11	17,4	19,2	18,3	Virocult
H12	17,2	19,6	18,4	Virocult
H13	17,3	19,5	18,4	Transwab
H14	17,8	20,7	19,25	Transwab
H15	18,4	20,7	19,55	Transwab
H16	18,3	21,2	19,75	Transwab
H17	19,3	20,3	19,8	Virocult
M1*	19.2	21.2	20.2	Virocult
M2*	19.4	21.6	20.5	Virocult
M3*	20.1	22.3	21.2	Transwab
M4*	20.1	22.5	21.3	Transwab
M5*	20.6	22.7	21.7	Virocult
M6*	20.8	23.2	22.0	Virocult
M7*	21.3	24.2	22.8	Virocult
M8*	21.6	24.2	22.9	Transwab
M9*	22.2	24.2	23.2	Virocult
M10*	22.1	24.7	23.4	Transwab
M11*	22.5	24.8	23.7	Transwab
M12*	23.4	25.3	24.4	Transwab
M13	19,3	21,1	20,2	Virocult
M14	19,5	21,5	20,5	Virocult
M15	19,6	22,1	20,85	Virocult
M16	19,7	22,2	20,95	Transwab
M17	19,8	22,3	21,05	Virocult
M18	20,6	22,7	21,65	Virocult
M19	21	23,1	22,05	Virocult
M20	21,4	23,8	22,6	Virocult
M21	22,9	24,9	23,9	Virocult
M22	23,1	25,5	24,3	Virocult
M23	23,3	26	24,65	Transwab
L1*	25.1	27.1	26.1	Transwab
L2*	25.1	27.4	26.3	Transwab
L3*	25.7	28.2	27.0	Transwab

Sample ID	Ct E	Ct N2	Average Ct	Medium
L4	24,3	26	25,15	Transwab
L5	24,2	26,3	25,25	Transwab
L6	24,3	26,2	25,25	Virocult
L7	24,1	26,4	25,25	Virocult
L8	24,6	27,2	25,9	Transwab
L9	24,4	27,5	25,95	Virocult
L10	25,6	27,6	26,6	Virocult
L11	25,4	27,9	26,65	Transwab
L12	26	28	27	Virocult
L13	25,6	28,4	27	ESwab
L14	26	28,1	27,05	Virocult
L15	26,3	28,1	27,2	Virocult
L16	26,3	28,1	27,2	Transwab
L17	26,2	28,4	27,3	Virocult
L18	26,1	28,6	27,35	Virocult
L19	26,4	28,6	27,5	Virocult
L20	26,5	29,9	28,2	ESwab
L21	27,1	29,6	28,35	Transwab
L22	27,1	29,7	28,4	Virocult
L23	27,1	29,7	28,4	Virocult
L24	27,1	29,8	28,45	Virocult
L25	27,3	30,1	28,7	Transwab
L26	27,6	30,2	28,9	Virocult
L27	28,2	30,4	29,3	Transwab
L28	28,3	30,3	29,3	Transwab
L29	28,5	30,4	29,45	Virocult
L30	28,8	30,5	29,65	Virocult
L31	28,3	31,2	29,75	Virocult
L32	28,4	31,2	29,8	Transwab
L33	28,8	30,9	29,85	Transwab
L34	28,5	31,5	30	Transwab
VL1	29,1	31,5	30,3	Transwab
VL2	29,1	31,6	30,35	Virocult
VL3	29,1	31,8	30,45	Transwab
VL4	29,4	32,8	31,1	Virocult
VL5	30	32,5	31,25	Transwab
VL6	29,9	32,7	31,3	Virocult
VL7	30,6	33,3	31,95	Virocult
VL8	30,7	34,2	32,45	Transwab
VL9	31,1	34,2	32,65	Virocult
VL10	31	34,6	32,8	Transwab
VL11	32,3	34,5	33,4	Virocult
VL12	32	34,8	33,4	Transwab
VL13	31,9	35,1	33,5	Virocult
VL14	32,2	35	33,6	Transwab
VL15	31,9	35,5	33,7	Transwab
VL16	32,7	34,8	33,75	Transwab
VL17	32,5	35,1	33,8	Transwab
VL18	32,4	35,7	34,05	Virocult
VL19	33,5	35,1	34,3	Transwab
VL20	33,5	35,3	34,4	Transwab
VL21	34,4	35,9	35,15	Virocult
VL22	33,8	36,7	35,25	Virocult
VL23	33,5	37,2	35,35	Transwab
VL24	33,9	37,3	35,6	Virocult
VL25	34,9	36,9	35,9	Virocult
VL26	34,5	37,4	35,95	Virocult
VL27	34,7	37,3	36	Virocult
VL28	34,4	37,6	36	Transwab
VL29	34,7	37,5	36,1	Virocult
VL30	35,5	36,8	36,15	Virocult
VL31	35,6	36,8	36,2	Transwab
VL32	35,2	37,6	36,4	Transwab
VL33	35,5	38	36,75	Transwab
VL34	35,1	38,8	36,95	Transwab
VL35	37,6	36,8	37,2	Transwab
VL36	36,4	39,4	37,9	Transwab
VL37	37	40,2	38,6	Virocult
VL38	38,7	40,1	39,4	Transwab
VL39	38,8	40,7	39,75	Virocult
VL40	42	38,2	40,1	Virocult

Sample ID	Ct E	Ct N2	Average Ct	Medium
VL41	40,1	41,1	40,6	Transwab
VL42	44,6	42,3	43,45	Transwab
N1*	NA	NA	NA	Virocult
N2*	NA	NA	NA	Virocult
N3*	NA	NA	NA	Virocult
N4*	NA	NA	NA	Virocult
N5*	NA	NA	NA	Transwab
N6*	NA	NA	NA	Transwab
N7	NA	NA	NA	Transwab
N8	NA	NA	NA	Transwab
N9	NA	NA	NA	Transwab
N10	NA	NA	NA	Transwab
N11	NA	NA	NA	Transwab
N12	NA	NA	NA	Transwab
N13	NA	NA	NA	Transwab
N14	NA	NA	NA	ESwab
N15	NA	NA	NA	Transwab
N16	NA	NA	NA	Virocult
N17	NA	NA	NA	Transwab
N18	NA	NA	NA	Transwab
N19	NA	NA	NA	Virocult
N20	NA	NA	NA	Transwab
N21	NA	NA	NA	ESwab
N22	NA	NA	NA	Transwab
N23	NA	NA	NA	Transwab
N24	NA	NA	NA	Transwab
N25	NA	NA	NA	Virocult
N26	NA	NA	NA	Virocult
N27	NA	NA	NA	Virocult
N28	NA	NA	NA	Transwab
N29	NA	NA	NA	Transwab
N30	NA	NA	NA	Transwab
N31	NA	NA	NA	Virocult
N32	NA	NA	NA	Transwab
N33	NA	NA	NA	Transwab
N34	NA	NA	NA	Virocult
N35	NA	NA	NA	Transwab
N36	NA	NA	NA	Virocult
N37	NA	NA	NA	Virocult
N38	NA	NA	NA	Virocult
N39	NA	NA	NA	Transwab
N40	NA	NA	NA	Transwab
N41	NA	NA	NA	Transwab

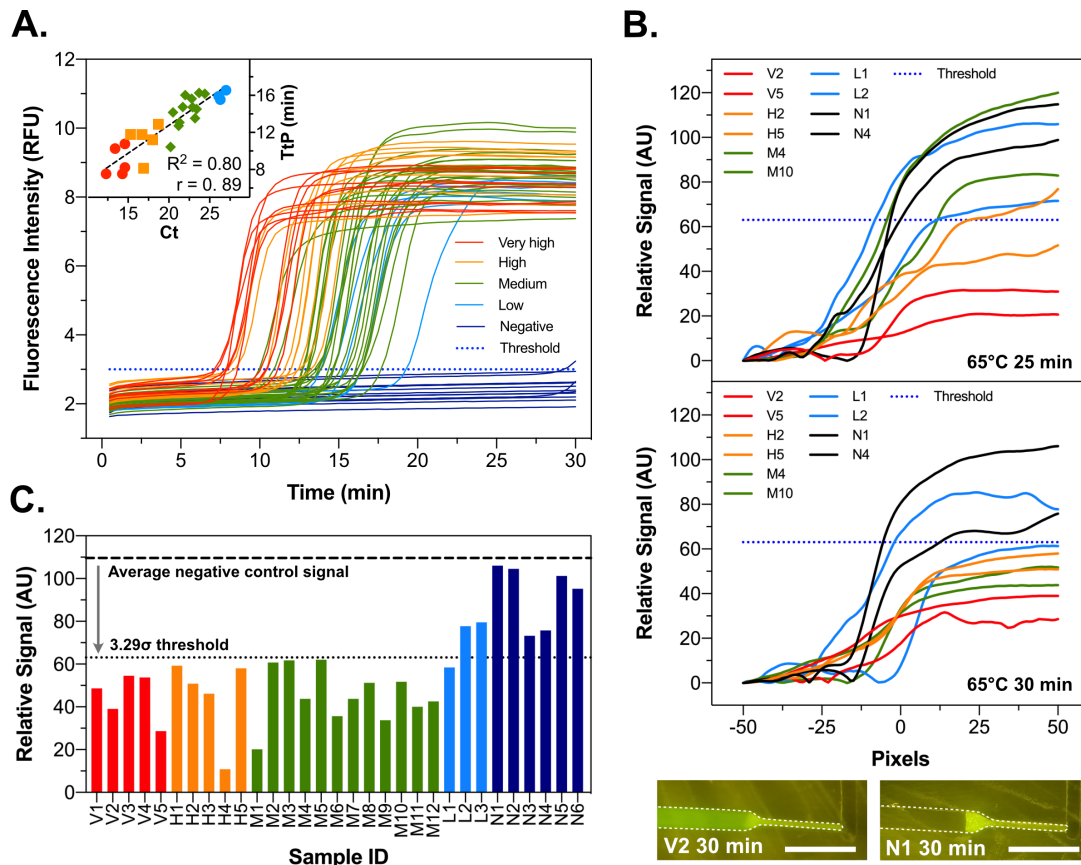


Figure S6. Detection of SARS-CoV-2 in heat inactivated nasopharyngeal swab samples using the iLACO primer set. The samples in Table 1 were grouped in 5 categories, namely (1) very high – average Ct <15 (red), (2) high – Ct between 20 and 15 (yellow), (3) medium – Ct between 20 and 25 (green), (4) low – Ct > 25 (blue) and (5) negative (dark blue). Color coding applies to A, B and C. **A-** RT-LAMP analysis of clinical samples using a benchtop real-time thermocycler (micPCR). All samples were measured in duplicate. The inset plot shows the correlation between average PCR Ct value of each sample and time to positivity (TtP) measured for RT-LAMP. TtP was determined as the required incubation time at 65°C to increase the fluorescence intensity above the threshold. The threshold was fixed as the highest background fluorescence (before amplification) measured among all tested samples. The r value is the Pearson correlation coefficient. **B-** Measurement of 2 samples in each Ct range using the integrated on-chip platform with an incubation time of 25 or 30 min at 65°C. Scale bars: 5 mm. **C-** Relative signal measured at pixel 50 for each nasopharyngeal swab sample. Relative values below the threshold are considered positive for SARS-CoV-2 RNA. The threshold and relative signal values in B and C were determined as previously described in section 2.3.

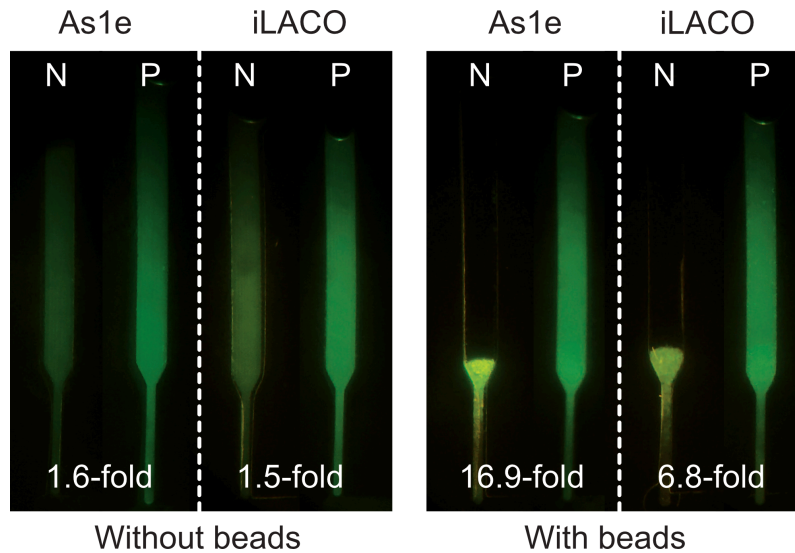


Figure S7. Comparison of positive to negative fluorescence ratio for each As1e and iLACO primer sets in the presence and absence of NBNM beads. All images were acquired on the disc (at room temperature) using a smartphone with a constant ISO of 800. In the case of the channels without the beads, the signal is quantified as average fluorescence, whereas for the channels with beads the fluorescence is quantified using a line profile at the bead-liquid interface as described in the manuscript. All signal quantifications were performed using only the green channel. The negative and positive samples were composed of RNase/DNase free water without or with 10^4 copies of SARS-CoV-2 full length synthetic RNA (Twist Bioscience, CA, USA, Control 2, GenBank: MN908947.3).

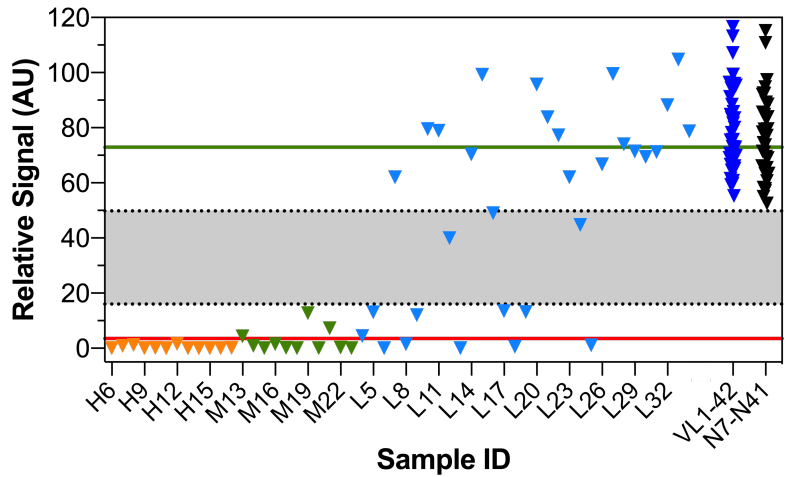


Figure S8. Detection of SARS-CoV-2 RNA in heat inactivated nasopharyngeal swab samples on the integrated platform (As1e primer set). Relative signal values were measured at pixel 50 according to section 2.3. Relative signal values above the gray band are considered negative while values below the gray band are considered positive. Values falling on the gray band are considered inconclusive. The upper and lower ranges of the grey band are calculated as 3.29σ (99.9% confidence interval threshold) of 9 independent measurements of negative and positive controls, respectively. Green and red lines indicate the mean relative signal of the negative and positive controls, respectively. The negative and positive controls were composed of RNase/DNase free water without or with 10^4 copies of SARS-CoV-2 full length synthetic RNA (Twist Bioscience, CA, USA, Control 2, GenBank: MN908947.3).

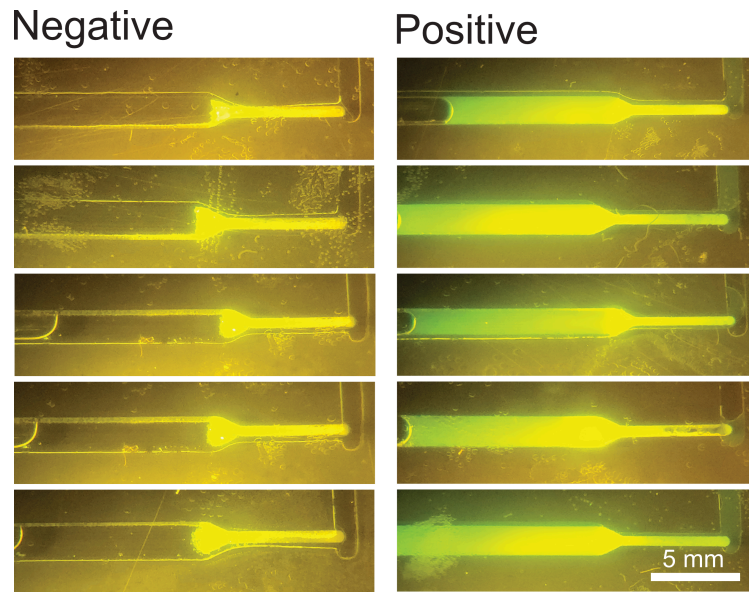


Figure S9. Representative raw smartphone photos taken on the integrated platform for five negative and five positive nasopharyngeal swab samples.

Table S2. Cost estimate of the key components required to assemble the integrated platform. PMMA sheets required to assemble the box and fabricate disposable discs are not included since prices are highly dependent on scale and expected to represent a small fraction of total production costs.

Item	Price (\$)	Quantity	Total (\$)
Silicone Heater Mat	50	2	100
Type K Thermocouple	6.8	2	13.6
Thermocouple Amplifier	18.3	2	36.6
IRF540PBF N-Channel MOSFET	1.3	2	2.6
Osram Opto PL 450B Blue Laser Diode	22	1	30
LM217LZ-TR Linear Voltage Regulator	0.4	1	0.4
Polyimide absorption filter	75 (5 sheets)	1/10 sheet	1.5
Bipolar Hall Effect Sensor	2.5	1	2.5
Arduino UNO	24	1	24
EMax 2204 + ESC (Motor)	24	1	24
Grand Total			235.2